

## Strongly Correlated Charge Density Wave in $\text{La}_{2-x}\text{Sr}_x\text{CuO}_4$ Evidenced by Doping-Dependent Phonon Anomaly

J. Q. Lin<sup>1,2,3,4</sup>, H. Miao<sup>1,‡</sup>, D. G. Mazzone<sup>1</sup>, G. D. Gu<sup>1</sup>, A. Nag<sup>5</sup>, A. C. Walters<sup>5</sup>, M. García-Fernández<sup>5</sup>, A. Barbour<sup>6</sup>, J. Pelliciani<sup>6</sup>, I. Jarrige<sup>6</sup>, M. Oda<sup>7</sup>, K. Kurosawa<sup>7</sup>, N. Momono<sup>8</sup>, Ke-Jin Zhou<sup>5</sup>, V. Bisogni<sup>6</sup>, X. Liu<sup>2,\*</sup> and M. P. M. Dean<sup>1,†</sup>

<sup>1</sup>Condensed Matter Physics and Materials Science Department, Brookhaven National Laboratory, Upton, New York 11973, USA

<sup>2</sup>School of Physical Science and Technology, ShanghaiTech University, Shanghai 201210, China

<sup>3</sup>Institute of Physics, Chinese Academy of Sciences, Beijing 100190, China

<sup>4</sup>University of Chinese Academy of Sciences, Beijing 100049, China

<sup>5</sup>Diamond Light Source, Harwell Campus, Didcot, Oxfordshire OX11 0DE, United Kingdom

<sup>6</sup>National Synchrotron Light Source II, Brookhaven National Laboratory, Upton, New York 11973, USA

<sup>7</sup>Department of Physics, Hokkaido University, Sapporo 060-0810, Japan

<sup>8</sup>Department of Sciences and Informatics, Muroran Institute of Technology, Muroran 050-8585, Japan

 (Received 11 January 2020; accepted 25 March 2020; published 21 May 2020)

The discovery of charge-density-wave-related effects in the resonant inelastic x-ray scattering spectra of cuprates holds the tantalizing promise of clarifying the interactions that stabilize the electronic order. Here, we report a comprehensive resonant inelastic x-ray scattering study of  $\text{La}_{2-x}\text{Sr}_x\text{CuO}_4$  finding that charge-density wave effects persist up to a remarkably high doping level of  $x = 0.21$  before disappearing at  $x = 0.25$ . The inelastic excitation spectra remain essentially unchanged with doping despite crossing a topological transition in the Fermi surface. This indicates that the spectra contain little or no direct coupling to electronic excitations near the Fermi surface, rather they are dominated by the resonant cross section for phonons and charge-density-wave-induced phonon softening. We interpret our results in terms of a charge-density wave that is generated by strong correlations and a phonon response that is driven by the charge-density-wave-induced modification of the lattice.

DOI: [10.1103/PhysRevLett.124.207005](https://doi.org/10.1103/PhysRevLett.124.207005)

Thirty years after the discovery of high-temperature superconductivity in the cuprates, there is still no consensus regarding the minimal set of interactions needed to describe the “normal state” from which superconductivity emerges [1]. Popular Hubbard and “ $t - J$ ” theoretical models suggest that superconducting, charge-density wave (CDW), and spin-density wave (SDW) states have similar ground state energies [2–9], which is consistent with experiments that reveal widespread interplay between all three states [10–16]. This complexity motivates experimental efforts to measure collective excitations associated with CDW order that should clarify the pertinent interactions. Resonant inelastic x-ray scattering (RIXS), as illustrated in Fig. 1(a), has an enhanced sensitivity to valence charge and phonon excitations [17]. Several experiments indeed reported anomalies in cuprate RIXS spectra at the CDW wave vector ( $\mathbf{Q}_{\text{CDW}}$ ), opening new routes to understand cuprate CDWs [18–23]. Uniquely isolating and interpreting CDW effects in RIXS is, however, complicated as CDWs inevitably modify their host crystal lattice and thus the phonons. Compounding this problem, RIXS spectra near  $\mathbf{Q}_{\text{CDW}}$  have been conceptualized in several different ways including charge excitations [21,22,24], momentum-dependent electron-phonon coupling (EPC) [23] and Fano effects [20].

In this Letter, we use ultrahigh energy-resolution RIXS to examine the nature of the CDW in  $\text{La}_{2-x}\text{Sr}_x\text{CuO}_4$  (LSCO). We observe that CDW correlations and associated CDW-induced phonon-softening persist up to a strikingly high doping level of  $x = 0.21$  before both effects disappear at  $x = 0.25$ . The large doping range  $x = 0.12 \rightarrow 0.25$  traverses a topological transition in the Fermi surface [25–27], allowing us to empirically test the relative importance of charge and lattice effects in the excitation spectra. We find that the data can be described entirely in terms of CDW-induced phonon softening and wave-vector-dependent changes in the phonon displacement, without invoking any more complex electronic excitations or CDW-related modification of the EPC. Overall, our results suggest a “real-space” picture in which the CDW emerges due to strong electronic correlations and modifies the underlying phonons.

LSCO single crystals with  $x = 0.12, 0.17, 0.21$ , and  $0.25$  were grown using the floating zone method and are denoted as LSCO $_n$  where  $n = 12, 17, 21$ , and  $25$ , respectively [28]. Structural and electronic characterization of the samples indicates excellent quality [27,28]. High energy-resolution RIXS measurements were performed at 2-ID at the National Synchrotron Light Source II, Brookhaven

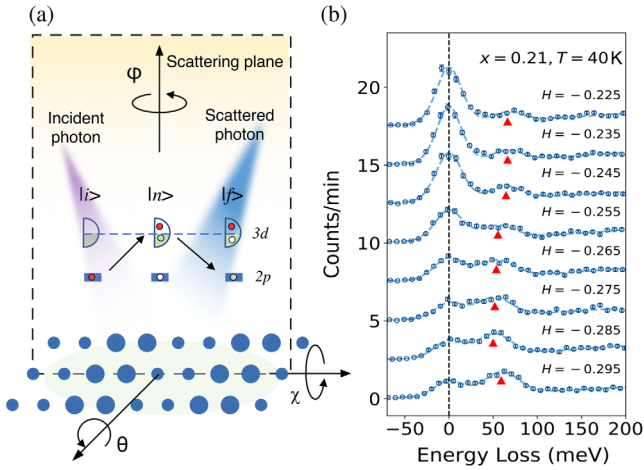


FIG. 1. RIXS process and typical low-energy RIXS spectra. (a) Schematic of the Cu  $L_3$ -edge RIXS process and experimental setup.  $|i\rangle$ ,  $|n\rangle$ , and  $|f\rangle$  represent initial, intermediate, and final states, respectively, and solid (empty) circles represent occupied (unoccupied) states.  $\theta$ ,  $\chi$ , and  $\phi$  denote the sample rotations. (b) High-resolution ( $\Delta E = 30$  meV) RIXS data for LSCO21 at  $T = 40$  K (blue circles) as a function of reciprocal lattice parameter  $H$  illustrating the principle components of the spectra: quasielastic scattering (marked by the vertical dotted line) and a low-energy phonon excitation (indicated by red triangles). The fit, as described in the main text, is represented by the dashed blue line.

National Laboratory with a resolution of  $\Delta E = 30$  meV full-width at half-maximum (FWHM) and a scattering angle of  $2\theta = 130^\circ$  and at I21 at Diamond Light Source featuring a resolution of  $\Delta E = 55$  meV and  $2\theta = 120^\circ$  [29].

The RIXS process is shown in Fig. 1(a). X-rays were tuned to the Cu  $L_3$  edge and measurements were taken with  $\sigma$  x-ray polarization perpendicular to the scattering plane (unless otherwise specified). Reciprocal lattice units (r.l.u.) are defined in terms of  $(H, K, L)$  with lattice constants  $a = b = 3.76$  Å,  $c = 13.28$  Å. Samples were aligned by optimizing the CDW intensity as a function of  $\phi$  in order to set a  $(H, 0, L)$  scattering plane for all data shown. Different values of  $H$  were accessed by rotating  $\theta$  without changing  $2\theta$  (i.e.,  $L$  varies with  $H$ ). Intensities were normalized to the intensity of the  $dd$  excitations similar to previous works [11,19,20,24]. Grazing incidence geometry (defined as negative  $H$ ) was chosen to enhance the intensity of charge and lattice (phonon) excitations, and to suppress spin excitations, which are, in any case,  $> 200$  meV and outside of the energy window we focus on in this Letter [30,31].

Figure 1(b) plots RIXS data of LSCO at the Cu  $L_3$  edge illustrating the main spectral features studied here: (i) a quasielastic peak and (ii) a dispersive feature around 50–65 meV. Feature (i) contains a component of trivial elastically scattered x-rays due to the finite disorder (defects) in the sample and surface scattering. Quasielastic scattering is further enhanced by static or quasistatic CDW correlations and displays a peak at  $Q_{\text{CDW}}$  whenever such correlations are present. The inelastic feature (ii) has been seen in several other cuprate RIXS experiments [20,22–24,32,33] and is assigned to the in-plane Cu-O bond-stretching (BS) phonon mode in agreement with early inelastic x-ray and neutron works [34–40]. The spectra were fitted with a pseudo-Voigt function for the elastic peak, an antisymmetric Lorentzian function for the BS mode and a linear background. All components of the fit were convoluted with the energy resolution function.

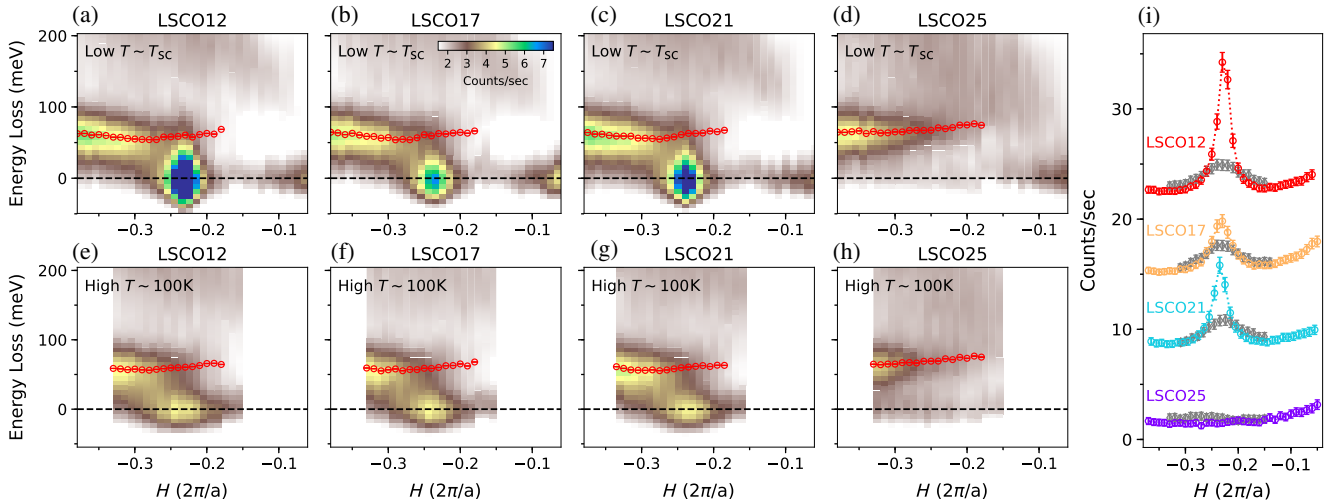


FIG. 2. Doping and temperature evolution. (a)–(d) show ( $\Delta E = 55$  meV) RIXS maps of  $\text{LSCO}_n$  ( $n = 12, 17, 21, 25$ ) at their superconducting transition temperature  $T_{\text{SC}}$  [28], where the CDW is strongest. All maps share the same colorscale inset in panel (b). Red circles represent the BS phonon energy. (e)–(h) The same measurement for  $T = 100$  K. (i) Comparison of integrated intensity in the  $\pm 20$  meV energy window. Data from panels (a)–(d) at  $T = T_{\text{SC}}$  are represented in color; data at  $T = 100$  K from panels (e)–(h) are plotted in gray.

Having assigned the basic spectral features, we use the ultra-high throughput of the I21 beam line to comprehensively map out the momentum and doping dependence of  $\text{LSCO}_n$   $12 \leq n \leq 25$ , (see Fig. 2). This doping range crosses over from  $1/8$  doping, where the CDW correlations are strongest, into the overdoped Fermi-liquid-like phase where the CDW disappears [25–27]. Importantly, this traverses a topological transition in the electronic structure where hole-pocket or Fermi-arc states transform into an electronlike Fermi surface with a more Fermi-liquid-like scattering rate [25–27,41]. This allows us to investigate the relationship of the RIXS spectra with the changes in electronic structure.

We first discuss the quasielastic CDW feature, which is summarized in Fig. 2(i), showing the integrated intensity in the  $\pm 20$  meV energy range of Figs. 2(a)–2(h). The intensity enhancement of the resonant process combined with the background suppression attained by energy-resolving the scattered beam make RIXS very sensitive to even very short correlation length CDWs. A CDW around an in-plane wave vector of  $(-0.23, 0)$  is not only observed for  $\text{LSCO}_{12}$ , where it was seen several times previously [15,16,42,43], but also up to far higher dopings of  $\text{LSCO}_{21}$  [44]. The  $H$ -width of the quasielastic scattering is consistent with correlation lengths (calculated as  $2/\text{FWHM}$ ) of 25–45 Å with shorter values for  $x = 0.17$ . Within error, the peaks exist at the same  $H_{\text{CDW}} = -0.231 \pm 0.005$  r.l.u., consistent with the stripe phenomenology where  $H_{\text{CDW}}$  saturates for  $x > 1/8$  [45]. As expected, a substantial fraction of the CDW intensity is suppressed upon warming to 100 K, leaving only a much weaker and diffuse signal [15,16,27]. We further observe a nonmonotonic intensity dependence as function of doping, with  $\text{LSCO}_{17}$  being weaker than  $\text{LSCO}_{12}$  and  $\text{LSCO}_{21}$ . There are multiple potential explanations for such a behavior. Perhaps most plausible is to note that the quasistatic CDW intensity in cuprates tends to compete with superconductivity, so the reduced CDW intensity at  $x = 0.17$  may be associated with the enhanced superconducting correlations that are known to exist at this near-optimal doping level.

Next we discuss the inelastic component of the spectra in Figs. 2(a)–2(h). In the 100–200 meV energy window, above the maximum phonon energy, flat, structure-less intensity arising from the charge continuum and the tail of the higher energy paramagnon excitations is present over all  $\mathbf{Q}$ . This intensity shows no clear changes around  $\mathbf{Q}_{\text{CDW}}$  and minimal changes with doping. In fact, only a slight increase in the overall intensity is found with increasing doping, which is expected as overdoped samples are more metallic. The inelastic intensity below 100 meV is dominated by the BS phonon, which shows clear energy dispersion and very strong intensity variation. To separate the phonon from charge and quasielastic intensity, we fit the data using the previously described model and display the results as red

circles in Figs. 2(a)–2(h). Since the phonon intensity drops strongly as  $|H|$  decreases, we focus on  $|H| > 0.18$  where the BS phonon can be fitted with good precision.

Figure 3 summarizes the evolution of the BS phonon parameters. Although the phonon softening, shown in Fig. 3(a), is appreciable ( $13 \pm 4$  meV or  $19 \pm 6\%$ ), it never shows full soft-mode (i.e., zero energy) behavior. The simultaneous disappearance of both the elastic peak and the phonon softening in  $\text{LSCO}_{25}$  makes a strong case that the softening is intimately related to the CDW correlations. Inelastic x-ray and neutron scattering measurements of phonon softening in underdoped cuprates have also assigned the phonon softening to CDW correlations [34–40]. It is noted that the phonon energy in  $\text{LSCO}_{25}$  is slightly higher than in other samples, which might be linked to lattice contraction associated with large Sr concentrations.

The phonon intensity dispersion is plotted in Fig. 3(c). Within error, no phonon intensity anomalies are seen around  $\mathbf{Q}_{\text{CDW}}$ , instead the clearest feature is a strong increase with  $|H|$ . Since RIXS excites phonons via the EPC process, the measured intensity reflects this interaction strength and scales with  $g^2$  where  $g$  is the EPC [17,32,33,46,47]. As a function of  $\mathbf{Q}$ , the “breathing-type” Cu-O bond displacement involved in the BS mode changes. Assuming a well-defined Madelung energy change associated with

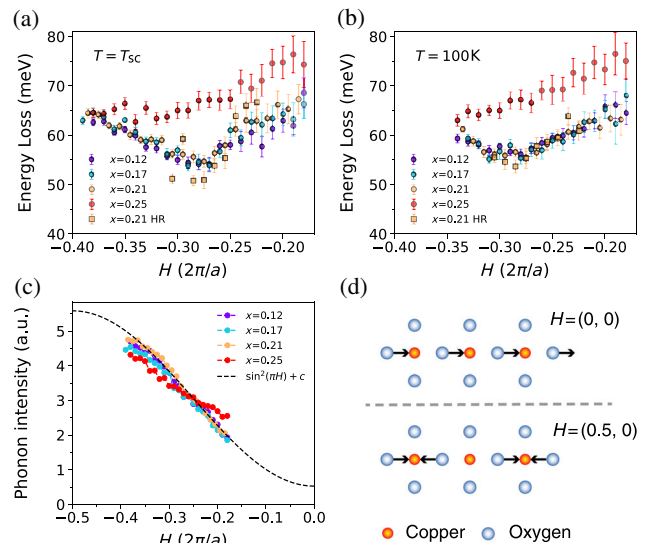


FIG. 3. Momentum dependent energy and intensity of the BS phonon mode. (a),(b) Show the phonon energy dispersion and softening in the vicinity of  $\mathbf{Q}_{\text{CDW}}$  at (a)  $T = T_{\text{SC}}$  and (b)  $T = 100$  K. Circles and squares represent data from Fig. 2 ( $\Delta E = 55$  meV) and Fig. 1 [with high-resolution (HR)  $\Delta E = 30$  meV], respectively. (c) Plots the integrated intensity of the BS phonon mode at  $T = T_{\text{SC}}$  in the [40, 120] meV energy window after subtracting elastic peak. The dashed line represents the  $\sin^2(\pi H) + \text{const}$  fit to  $\text{LSCO}_{21}$ . (d) Illustration of the oxygen atom displacements involved in the BS mode at  $H = (0, 0)$  and  $(0.5, 0)$ .

Cu-O bond stretching, one can predict RIXS intensity scaling  $I \propto g_{\text{br}}^2 = \sin^2(\pi H) + \sin^2(\pi K)$  [32,33,46,48]. The comparison in Fig. 3(c) shows that this simple model is sufficient to describe the intensity behavior of our data, without invoking any more complex phenomenology. It is worth adding that definitively distinguishing  $\sin^2(\pi H)$  scaling from other scaling forms is somewhat challenging. The photon energy corresponding to the Cu  $L_3$  edge intrinsically limits the highest  $|H|$  we can reach, and at low  $|H|$  leakage of specular scattering intensity overwhelms the low-energy region of the RIXS spectra. The slight flattening of the dispersion at  $x = 0.25$  might arise from some leakage of additional background at high doping levels. With these considered, the agreement with  $\sin^2(\pi H)$  scaling holds well in the reciprocal-space range measured.

*Discussion of the CDW.*—Both the quasielastic RIXS intensity and the phonon softening demonstrate the existence of CDW correlations up to a remarkably high doping level of  $x = 0.21$ , traversing the topological transition in the electronic structure [25–27], in which arc or hole-pocket-like states centered around the Brillouin zone corner transform into an electron-like Fermi surface at the Brillouin zone center. This result confirms very recent non-resonant diffraction measurements and shows, due to the resonant nature of the RIXS probe, that the correlations involve the electronically active Cu states [27]. The persistence of the CDW correlations, despite very substantial Fermi surface changes, provides a vivid demonstration that the LSCO CDW cannot be described using any type of weak-coupling Fermi surface nesting picture, as previously suggested for some other cuprate materials [49]. It is also notable that our results show no clear phonon intensity changes around  $\mathbf{Q}_{\text{CDW}}$ , which argues against the CDW-related modification of electron-phonon coupling, which has been proposed as a CDW formation mechanisms in other studies [23]. Instead, the nearly doping-independent CDW wave vector supports mechanisms in which the periodicity of the CDW is set by the short-range electronic interactions. Here, doped holes can save super-exchange energy by clustering together and breaking fewer magnetic bonds, but by doing so, they pay a cost of increased kinetic and Coulomb energy. It has been proposed that a CDW is the optimal compromise between these two tendencies [4]. However, a fascinating question remains regarding why the CDW is so stable against increasing doping and electron itineracy.

Our results motivate a reexamination of the anomalous transport properties of the cuprates, which are often discussed in terms of strange metal physics below a critical doping level of  $x_c \approx 0.19$ , where the systems becomes increasingly more Fermi-liquid-like [1]. Since CDW correlations can exist over a more extended doping range than previously thought, it is interesting to consider their influence on transport properties [50]. These results, however, argue against a quantum critical point that is

associated with a CDW transition as similar as CDW correlations exist in LSCO17 and LSCO21, either side of the putative critical doping of  $x_c \approx 0.19$ . In terms of the CDW fluctuations, we note that the size of the phonon softening is reduced when warming to  $T = 100$  K, but the magnitude of the reduction is considerably less than the reduction in the quasielastic CDW intensity. This suggests that only a relatively small fraction of the total CDW correlations are nucleated into the CDW order, as otherwise the magnitude of the phonon softening would be expected to scale with the quasielastic intensity.

An intriguing feature of the CDW effects is that the  $\mathbf{Q}$  vector with the largest phonon softening does not coincide with the peak in the quasielastic scattering at 0.235 r.l.u., but occurs at a larger wave vector of  $H = 0.275$  r.l.u. We can consider two candidate explanations for this. The first is that the interactions causing the CDW instability are not the same as the interactions that pin the CDW. Electronic interactions, for instance, may potentially stabilize a wide range of CDW wave vectors, but lattice or SDW coupling might play the final role in setting the final CDW wave-vector. This concept was proposed several years ago [51] and is further supported by the previously observed change in CDW wave vector with temperature [19,24,52]. The phonon softening does not show any obvious difference between  $T_{\text{SC}}$  and 100 K in Figs. 3(a) and 3(b), in contrast to the intensity of the elastic scattering from the CDW peak, which also supports distinct mechanisms for CDW formation and CDW pinning. Another potential explanation for the shift is that the effect is due to the  $\mathbf{Q}$  dependence of the EPC. Since EPC increases with  $H$ , the softening at higher  $H$  will be enhanced, which would displace the point of maximum softening.

*Discussion of electronic CDW excitations.*—A strength of the current dataset is the opportunity to compare LSCO12 and LSCO21, which exhibit comparable levels of CDW order, despite their very different doping levels. Any electronic CDW excitations that may be present in the RIXS spectra would be expected to increase with electronic density of states and change substantially with doping. Since the overall form of the spectra is rather similar over this large doping range, our results argue against the presence of electronic CDW excitations, as suggested previously, as a ubiquitous, intrinsic feature of RIXS spectra of the cuprates [20]. It is, however, possible that the x-ray polarization is important to observing electronic CDW excitations [53].

*Electron phonon coupling.*—The concept of using RIXS to extract EPC in cuprates has generated considerable excitement recently [23,32,33,46,54]. Our results support this, in the sense that we observe intensity scaling as  $I \propto \sin^2(\pi H)$ . However, no phonon intensity anomalies related to the CDW are observed. A recent preprint reports measurements of  $\text{La}_{1.8-x}\text{Eu}_{0.2}\text{Sr}_x\text{CuO}_{4+\delta}$  which used an incident energy detuning method, formulated in Refs. [32,33,54], to suggest

a very large CDW-induced modification of the EPC from  $g = 0.30 \rightarrow 0.35$  upon cooling into the CDW phase [23]. Assuming  $I \propto g^2$ , this would imply a phonon intensity change of  $(0.35/0.3)^2 \sim 1.4$ , when either cooling into the CDW phase or scanning through  $Q_{\text{CDW}}$ . As such, it is very difficult to justify the absence of a discernible  $\sim 40\%$  temperature-induced change in the phonon intensity at  $Q_{\text{CDW}}$  on resonance in our data or that in Ref. [23].

*RIXS as a probe of cuprate CDWs.*—Overall, our results support a real-space picture of an electronically driven CDW, without needing to invoke nesting or a van Hove singularity. RIXS measures the phonon softening occurring due to the charge modulation, but the overall doping dependence is fully explicable without invoking more complex phason, Fano, or CDW-enhanced EPC effects that have generated considerable excitement recently [18–21,23]. Our observation is backed, by improved energy resolution ( $\Delta E = 30$  meV) and more extensive doping dependence compared with what has been done previously [21,23–18]]. Excluding these exciting effects is at some level disappointing in terms of novel excitations, but is, however, highly important in view of the more-and-more extensive use of RIXS. Although RIXS, in this case, provides information similar to inelastic x-ray and neutron scattering, compelling applications for RIXS remain in cases where the x-ray penetration depth and resonant mode selectivity is important [47].

In conclusion, we report RIXS measurements of CDW correlations in LSCO over an extensive doping range. CDW-related quasielastic scattering and phonon softening is observed from  $x = 0.12$  to  $x = 0.21$ , traversing a topological transition in the Fermi surface, before disappearing at  $x = 0.25$ . Based on these results, we conclude that the spectra have little or no direct coupling to electronic excitations. Instead the spectra are dominated by CDW-driven phonon softening and phonon intensity variations arising from changes in the phonon displacement as a function of  $Q$ . Overall, our results support a scenario in which the CDW is driven by strong correlations and clarify that the low-energy RIXS response in cuprates is driven by the CDW modifying the lattice, without invoking more complex interactions.

This material is based upon work supported by the U.S. Department of Energy, Office of Basic Energy Sciences. Work at Brookhaven National Laboratory was supported by the U.S. Department of Energy, Office of Science, Office of Basic Energy Sciences, under Contract No. DE-SC0012704. X-ray research by M. P. M. D., D. G. M. and H. M. was supported by Field Work Proposal No. 23357. Data interpretation by X. L. at ShanghaiTech University, and J. Q. L.'s training as a graduate student were supported by the ShanghaiTech University startup fund, MOST of China under Grant No. 2016YFA0401000, NSFC under Grant No. 11934017 and the Chinese Academy of Sciences under Grant No. 112111KYSB20170059. The research by

V. B. was supported by the U.S. Department of Energy, Office of Basic Energy Sciences, Early Career Award Program. This research used resources at the Soft Inelastic X-Ray beamline of the National Synchrotron Light Source II, a U.S. Department of Energy (DOE) Office of Science User Facility operated for the DOE Office of Science by Brookhaven National Laboratory under Contract No. DE-SC0012704. We acknowledge Diamond Light Source for time on Beamline I21 under Proposal 22261.

\*liuxr@shanghaitech.edu.cn

†mdean@bnl.gov

‡Present address: Materials Science and Technology Division, Oak Ridge National Laboratory, Oak Ridge, Tennessee 37831, USA.

- [1] B. Keimer, S. A. Kivelson, M. R. Norman, S. Uchida, and J. Zaanen, From quantum matter to high-temperature superconductivity in copper oxides, *Nature (London)* **518**, 179 (2015).
- [2] J. Zaanen and O. Gunnarsson, Charged magnetic domain lines and the magnetism of high- $T_c$  oxides, *Phys. Rev. B* **40**, 7391 (1989).
- [3] D. Poilblanc and T. M. Rice, Charged solitons in the Hartree-Fock approximation to the large- $U$  Hubbard model, *Phys. Rev. B* **39**, 9749 (1989).
- [4] V. J. Emery, S. A. Kivelson, and H. Q. Lin, Phase Separation in the  $t$ - $J$  Model, *Phys. Rev. Lett.* **64**, 475 (1990).
- [5] K. Machida, Magnetism in  $\text{La}_2\text{CuO}_4$  based compounds. *Phys. C Supercond.* **158**, 196 (1989).
- [6] C. Castellani, C. Di Castro, and M. Grilli, Singular Quasiparticle Scattering in the Proximity of Charge Instabilities, *Phys. Rev. Lett.* **75**, 4650 (1995).
- [7] P. Corboz, T. M. Rice, and M. Troyer, Competing States in the  $t$ - $J$  Model: Uniform  $d$ -Wave State Versus Stripe State, *Phys. Rev. Lett.* **113**, 046402 (2014).
- [8] E. W. Huang, C. B. Mendl, S. Liu, S. Johnston, H.-C. Jiang, B. Moritz, and T. P. Devereaux, Numerical evidence of fluctuating stripes in the normal state of high- $T_c$  cuprate superconductors, *Science* **358**, 1161 (2017).
- [9] B.-X. Zheng, C.-M. Chung, P. Corboz, G. Ehlers, M.-P. Qin, R. M. Noack, H. Shi, S. R. White, S. Zhang, and G. K.-L. Chan, Stripe order in the underdoped region of the two-dimensional Hubbard model, *Science* **358**, 1155 (2017).
- [10] J. M. Tranquada, B. J. Sternlieb, J. D. Axe, Y. Nakamura, and S. Uchida, Evidence for stripe correlations of spins and holes in copper oxide superconductors, *Nature (London)* **375**, 561 (1995).
- [11] G. Ghiringhelli, M. Le Tacon, M. Minola, S. Blanco-Canosa, C. Mazzoli, N. B. Brookes, G. M. De Luca, A. Frano, D. G. Hawthorn, F. He, T. Loew, M. Moretti Sala, D. C. Peets, M. Salluzzo, E. Schierle, R. Sutarto, G. A. Sawatzky, E. Weschke, B. Keimer, and L. Braicovich, Long-range incommensurate charge fluctuations in  $(\text{Y}, \text{Nd})\text{Ba}_2\text{Cu}_3\text{O}_{6+x}$ , *Science* **337**, 821 (2012).
- [12] S. Blanco-Canosa, A. Frano, E. Schierle, J. Porras, T. Loew, M. Minola, M. Bluschke, E. Weschke, B. Keimer, and M. Le Tacon, Resonant x-ray scattering study of charge-density

- wave correlations in  $\text{YBa}_2\text{Cu}_3\text{O}_{6+x}$ , *Phys. Rev. B* **90**, 054513 (2014).
- [13] W. Tabis *et al.*, Synchrotron x-ray scattering study of charge-density-wave order in  $\text{HgBa}_2\text{CuO}_{4+\delta}$ , *Phys. Rev. B* **96**, 134510 (2017).
- [14] R. Comin, A. Frano, M. M. Yee, Y. Yoshida, H. Eisaki, E. Schierle, E. Weschke, R. Sutarto, F. He, A. Soumyanarayanan, Y. He, M. Le Tacon, I. S. Elfimov, J. E. Hoffman, G. A. Sawatzky, B. Keimer, and A. Damascelli, Charge order driven by Fermi-Arc instability in  $\text{Bi}_2\text{Sr}_{2-x}\text{La}_x\text{CuO}_{6+\delta}$ , *Science* **343**, 390 (2014).
- [15] T. P. Croft, C. Lester, M. S. Senn, A. Bombardi, and S. M. Hayden, Charge density wave fluctuations in  $\text{La}_{2-x}\text{Sr}_x\text{CuO}_4$  and their competition with superconductivity, *Phys. Rev. B* **89**, 224513 (2014).
- [16] V. Thampy, M. P. M. Dean, N. B. Christensen, L. Steinke, Z. Islam, M. Oda, M. Ido, N. Momono, S. B. Wilkins, and J. P. Hill, Rotated stripe order and its competition with superconductivity in  $\text{La}_{1.88}\text{Sr}_{0.12}\text{CuO}_4$ , *Phys. Rev. B* **90**, 100510(R) (2014).
- [17] L. J. P. Ament, M. van Veenendaal, T. P. Devereaux, J. P. Hill, and J. van den Brink, Resonant inelastic x-ray scattering studies of elementary excitations, *Rev. Mod. Phys.* **83**, 705 (2011).
- [18] M. P. M. Dean, G. Dellea, M. Minola, S. B. Wilkins, R. M. Konik, G. D. Gu, M. Le Tacon, N. B. Brookes, F. Yakhou-Harris, K. Kummer, J. P. Hill, L. Braicovich, and G. Ghiringhelli, Magnetic excitations in stripe-ordered  $\text{La}_{1.875}\text{Ba}_{0.125}\text{CuO}_4$  studied using resonant inelastic x-ray scattering, *Phys. Rev. B* **88**, 020403(R) (2013).
- [19] H. Miao, J. Lorenzana, G. Seibold, Y. Y. Peng, A. Amorese, F. Yakhou-Harris, K. Kummer, N. B. Brookes, R. M. Konik, V. Thampy, G. D. Gu, G. Ghiringhelli, L. Braicovich, and M. P. M. Dean, High-temperature charge density wave correlations in  $\text{La}_{1.875}\text{Ba}_{0.125}\text{CuO}_4$  without spin-charge locking, *Proc. Natl. Acad. Sci. U.S.A.* **114**, 12430 (2017).
- [20] L. Chaix, G. Ghiringhelli, Y. Y. Peng, M. Hashimoto, B. Moritz, K. Kummer, N. B. Brookes, Y. He, S. Chen, S. Ishida, Y. Yoshida, H. Eisaki, M. Salluzzo, L. Braicovich, Z.-X. Shen, T. P. Devereaux, and W.-S. Lee, Dispersive charge density wave excitations in  $\text{Bi}_2\text{Sr}_2\text{CaCu}_2\text{O}_{8+\delta}$ , *Nat. Phys.* **13**, 952 (2017).
- [21] R. Arpaia, S. Caprara, R. Fumagalli, G. De Vecchi, Y. Y. Peng, E. Andersson, D. Betto, G. M. De Luca, N. B. Brookes, F. Lombardi, M. Salluzzo, L. Braicovich, C. Di Castro, M. Grilli, and G. Ghiringhelli, Dynamical charge density fluctuations pervading the phase diagram of a Cu-based high- $T_c$  superconductor, *Science* **365**, 906 (2019).
- [22] B. Yu, W. Tabis, I. Bialo, F. Yakhou, N. Brookes, Z. Anderson, Y. Tang, G. Yu, and M. Greven, Unusual dynamic charge-density-wave correlations in  $\text{HgBa}_2\text{CuO}_{4+\delta}$ , [arXiv:1907.10047](https://arxiv.org/abs/1907.10047).
- [23] Y. Y. Peng, A. A. Husain, M. Mitrano, S. Sun, T. A. Johnson, A. V. Zakrzewski, G. J. MacDougall, A. Barbour, I. Jarrige, V. Bisogni, and P. Abbamonte, Enhanced electron-phonon coupling for charge-density-wave formation in  $\text{La}_{1.8-x}\text{Eu}_{0.2}\text{Sr}_x\text{CuO}_{4+\delta}$ , [arXiv:1910.05526](https://arxiv.org/abs/1910.05526).
- [24] H. Miao, R. Fumagalli, M. Rossi, J. Lorenzana, G. Seibold, F. Yakhou-Harris, K. Kummer, N. B. Brookes, G. D. Gu, L. Braicovich, G. Ghiringhelli, and M. P. M. Dean, Formation of Incommensurate Charge Density Waves in Cuprates, *Phys. Rev. X* **9**, 031042 (2019).
- [25] T. Yoshida, X. J. Zhou, K. Tanaka, W. L. Yang, Z. Hussain, Z.-X. Shen, A. Fujimori, S. Sahrakorpi, M. Lindroos, R. S. Markiewicz, A. Bansil, Seiki Komiyama, Yoichi Ando, H. Eisaki, T. Kakeshita, and S. Uchida, Systematic doping evolution of the underlying Fermi surface of  $\text{La}_{2-x}\text{Sr}_x\text{CuO}_4$ , *Phys. Rev. B* **74**, 224510 (2006).
- [26] M. Horio *et al.*, Three-Dimensional Fermi Surface of Overdoped La-Based Cuprates, *Phys. Rev. Lett.* **121**, 077004 (2018).
- [27] H. Miao, G. Fabbri, C. S. Nelson, R. Acevedo-Esteves, Y. Li, G. D. Gu, T. Yilmaz, K. Kaznatcheev, E. Vescovo, M. Oda, K. Kurosawa, N. Momono, T. A. Assefa, I. K. Robinson, J. M. Tranquada, P. D. Johnson, and M. P. M. Dean, Discovery of charge density waves in cuprate superconductors up to the critical doping and beyond, [arXiv:2001.10294](https://arxiv.org/abs/2001.10294).
- [28] See the Supplemental Material at <http://link.aps.org/supplemental/10.1103/PhysRevLett.124.207005> for sample synthesis, sample characterization, temperature-dependent phonon intensity data, and fitting of the RIXS spectra.
- [29] A scattering angle of  $2\theta = 120^\circ$  was chosen to access the CDW at  $L = 1.5$ , such that its intensity was maximized. Since the spectrometer at the National Synchrotron Light Source II was not continuously rotatable,  $2\theta = 130^\circ$  was chosen in order as a good compromise. Since the CDW is very broad in  $L$  this constitutes a minor difference.
- [30] M. P. M. Dean, G. Dellea, R. S. Springell, F. Yakhou-Harris, K. Kummer, N. B. Brookes, X. Liu, Y.-J. Sun, J. Strle, T. Schmitt, L. Braicovich, G. Ghiringhelli, I. Bozovic, and J. P. Hill, Persistence of magnetic excitations in  $\text{La}_{2-x}\text{Sr}_x\text{CuO}_4$  from the undoped insulator to the heavily overdoped non-superconducting metal, *Nat. Mater.* **12**, 1019 (2013).
- [31] D. Meyers, H. Miao, A. C. Walters, V. Bisogni, R. S. Springell, M. d'Astuto, M. Dantz, J. Pelliciani, H. Y. Huang, J. Okamoto, D. J. Huang, J. P. Hill, X. He, I. Božović, T. Schmitt, and M. P. M. Dean, Doping dependence of the magnetic excitations in  $\text{La}_{2-x}\text{Sr}_x\text{CuO}_4$ , *Phys. Rev. B* **95**, 075139 (2017).
- [32] L. Braicovich, M. Rossi, R. Fumagalli, Y. Peng, Y. Wang, R. Arpaia, D. Betto, G. M. De Luca, D. Di Castro, K. Kummer, M. Moretti Sala, M. Pagetti, G. Balestrino, N. B. Brookes, M. Salluzzo, S. Johnston, J. van den Brink, and G. Ghiringhelli, Determining the Electron-Phonon Coupling in Superconducting Cuprates by Resonant Inelastic X-ray Scattering: Methods and Results on  $\text{Nd}_{1+x}\text{Ba}_{2-x}\text{Cu}_3\text{O}_{7-\delta}$ , [arXiv:1906.01270](https://arxiv.org/abs/1906.01270).
- [33] M. Rossi, R. Arpaia, R. Fumagalli, M. Moretti Sala, D. Betto, K. Kummer, G. M. De Luca, J. van den Brink, M. Salluzzo, N. B. Brookes, L. Braicovich, and G. Ghiringhelli, Experimental Determination of Momentum-Resolved Electron-Phonon Coupling, *Phys. Rev. Lett.* **123**, 027001 (2019).
- [34] T. Fukuda, J. Mizuki, K. Ikeuchi, K. Yamada, A. Q. R. Baron, and S. Tsutsui, Doping dependence of softening in the bond-stretching phonon mode of  $\text{La}_{2-x}\text{Sr}_x\text{CuO}_4$   $0 \leq x \leq 0.29$ , *Phys. Rev. B* **71**, 060501(R) (2005).
- [35] D. Reznik, L. Pintschovius, M. Ito, S. Iikubo, M. Sato, H. Goka, M. Fujita, K. Yamada, G. D. Gu, and

- J. M. Tranquada, Electron-phonon coupling reflecting dynamic charge inhomogeneity in copper oxide superconductors, *Nature (London)* **440**, 1170 (2006).
- [36] J. Graf, M. d'Astuto, P. Giura, A. Shukla, N. L. Saini, A. Bossak, M. Krisch, S.-W. Cheong, T. Sasagawa, and A. Lanzara, In-plane copper-oxygen bond-stretching mode anomaly in underdoped  $\text{La}_{2-x}\text{Sr}_x\text{CuO}_{4+\delta}$  measured with high-resolution inelastic x-ray scattering, *Phys. Rev. B* **76**, 172507 (2007).
- [37] S. R. Park, T. Fukuda, A. Hamann, D. Lamago, L. Pintschovius, M. Fujita, K. Yamada, and D. Reznik, Evidence for a charge collective mode associated with superconductivity in copper oxides from neutron and x-ray scattering measurements of  $\text{La}_{2-x}\text{Sr}_x\text{CuO}_4$ , *Phys. Rev. B* **89**, 020506(R) (2014).
- [38] D. Reznik, L. Pintschovius, M. Fujita, K. Yamada, G. D. Gu, and J. M. Tranquada, Electron-phonon anomaly related to charge stripes: Static stripe phase versus optimally doped superconducting  $\text{La}_{1.85}\text{Sr}_{0.15}\text{CuO}_4$ , *J. Low Temp. Phys.* **147**, 353 (2007).
- [39] L. Pintschovius, D. Reznik, and K. Yamada, Oxygen phonon branches in overdoped  $\text{La}_{1.7}\text{Sr}_{0.3}\text{CuO}_4$ , *Phys. Rev. B* **74**, 174514 (2006).
- [40] L. Pintschovius and M. Braden, Anomalous dispersion of LO phonons in  $\text{La}_{1.85}\text{Sr}_{0.15}\text{CuO}_4$ , *Phys. Rev. B* **60**, R15039 (1999).
- [41] R. A. Cooper, Y. Wang, B. Vignolle, O. J. Lipscombe, S. M. Hayden, Y. Tanabe, T. Adachi, Y. Koike, M. Nohara, H. Takagi, C. Proust, and N. E. Hussey, Anomalous criticality in the electrical resistivity of  $\text{La}_{2-x}\text{Sr}_x\text{CuO}_4$ , *Science* **323**, 603 (2009).
- [42] H.-H. Wu, M. Buchholz, C. Trabant, C. F. Chang, A. C. Komarek, F. Heigl, M. V. Zimmermann, M. Cwik, F. Nakamura, M. Braden *et al.*, Charge stripe order near the surface of 12-percent doped  $\text{La}_{2-x}\text{Sr}_x\text{CuO}_4$ , *Nat. Commun.* **3**, 1023 (2012).
- [43] J.-J. Wen, H. Huang, S.-J. Lee, H. Jang, J. Knight, Y. S. Lee, M. Fujita, K. M. Suzuki, S. Asano, S. A. Kivelson, C.-C. Kao, and J.-S. Lee, Observation of two types of charge-density-wave orders in superconducting  $\text{La}_{2-x}\text{Sr}_x\text{CuO}_4$ , *Nat. Commun.* **10**, 3269 (2019).
- [44] These RIXS results are confirmed by bulk sensitive hard (8 keV) x-ray diffraction measurement under review [27].
- [45] K. Yamada, C. H. Lee, K. Kurahashi, J. Wada, S. Wakimoto, S. Ueki, H. Kimura, Y. Endoh, S. Hosoya, G. Shirane, R. J. Birgeneau, M. Greven, M. A. Kastner, and Y. J. Kim, Doping dependence of the spatially modulated dynamical spin correlations and the superconducting-transition temperature in  $\text{La}_{2-x}\text{Sr}_x\text{CuO}_4$ , *Phys. Rev. B* **57**, 6165 (1998).
- [46] T. P. Devereaux, A. M. Shvaika, K. Wu, K. Wohlfeld, C. J. Jia, Y. Wang, B. Moritz, L. Chaix, W.-S. Lee, Z.-X. Shen, G. Ghiringhelli, and L. Braicovich, Directly Characterizing the Relative Strength and Momentum Dependence of Electron-Phonon Coupling Using Resonant Inelastic X-Ray Scattering, *Phys. Rev. X* **6**, 041019 (2016).
- [47] D. Meyers *et al.*, Decoupling Carrier Concentration and Electron-Phonon Coupling in Oxide Heterostructures Observed with Resonant Inelastic X-Ray Scattering, *Phys. Rev. Lett.* **121**, 236802 (2018).
- [48] S. Johnston, F. Vernay, B. Moritz, Z.-X. Shen, N. Nagaosa, J. Zaanen, and T. P. Devereaux, Systematic study of electron-phonon coupling to oxygen modes across the cuprates, *Phys. Rev. B* **82**, 064513 (2010).
- [49] R. Comin and A. Damascelli, Resonant x-ray scattering studies of charge order in cuprates, *Annu. Rev. Condens. Matter Phys.* **7**, 369 (2016).
- [50] G. Seibold, R. Arpaia, Y. Y. Peng, R. Fumagalli, L. Braicovich, C. Di Castro, M. Grilli, G. Ghiringhelli, and S. Caprara, Marginal Fermi liquid behaviour from charge density fluctuations in cuprates, [arXiv:1905.10232](https://arxiv.org/abs/1905.10232).
- [51] O. Zachar, S. A. Kivelson, and V. J. Emery, Landau theory of stripe phases in cuprates and nickelates, *Phys. Rev. B* **57**, 1422 (1998).
- [52] H. Miao, D. Ishikawa, R. Heid, M. Le Tacon, G. Fabbris, D. Meyers, G. D. Gu, A. Q. R. Baron, and M. P. M. Dean, Incommensurate Phonon Anomaly and the Nature of Charge Density Waves in Cuprates, *Phys. Rev. X* **8**, 011008 (2018).
- [53] Data in Ref. [20] is taken with positive  $H$  (grazing exit geometry), distinct from the negative  $H$  (grazing incidence geometry).
- [54] L. J. P. Ament, M. Van Veenendaal, and J. Van Den Brink, Determining the electron-phonon coupling strength from resonant inelastic x-ray scattering at transition metal  $L$ -edges, *Europhys. Lett.* **95**, 27008 (2011).